# SUPPLEMENTARY INFORMATION

# Boron-Based Ternary $Rb_6Be_2B_6$ Cluster Featuring Unique Sandwich Geometry and Naked Hexagonal Boron Ring†

Ying-Jin Wang,*[ab] Lin-Yan Feng,[b] Li Xu,[a] Xiang-Ru Hou,[a] Nan Li,[a]

Chang-Qing Miao,[a] and Hua-Jin Zhai*[b]

[a]*Department of Chemistry, Xinzhou Teachers University, Xinzhou 034000, Shanxi, China*

[b]*Nanocluster Laboratory, Institute of Molecular Science, Shanxi University, Taiyuan 030006, China*

*E-mail: yingjinwang@sxu.edu.cn; hj.zhai@sxu.edu.cn

## Supplementary Information – Part I

**Table S1.** Cartesian coordinates for selected optimized structures of $Rb_6Be_2B_6$ cluster at the PBE0/def2-qzvp level: the $D_{3d}$ ($^1A_{1g}$) global-minimum (GM) *versus* the $TS_1$ ($D_{3d}$, $^1A_{1g}$) and $TS_2$ ($D_{3h}$, $^1A_1'$) transition states (TSs).

**Figure S1.** Alternative optimized low-lying structures of $Rb_6Be_2B_6$ cluster. Relative energies are shown in square brackets at the PBE0/def2-qzvp level with corrections for zero-point energies (ZPEs). Also shown are the relative energies for top five isomers at the single-point CCSD(T)/def2-qzvp//PBE0/def2-qzvp level. All energies are in eV.

**Figure S2.** Two different σ bonding schemes for the $BeRb_3$ ligands in GM $D_{3d}$ ($^1A_{1g}$) $Rb_6Be_2B_6$ cluster on the basis of adaptive natural density partitioning (AdNDP) analysis. Occupation numbers (ONs) are indicated. The three-center two-electron (3c-2e) σ scheme in (b) gives a relatively low ON value, indicating that the σ

bond is entirely delocalized within the tetrahedral $BeRb_3$ unit as presented in the 4c-2e σ scheme in (a).

**Figure S3.** Comparison of the delocalized π/σ sextets of (a) $D_{3d}$ ($^1A_{1g}$) GM $Rb_6Be_2B_6$ cluster with those of (b) model $D_{6h}$ $C_6$ cluster and (c) benzene.

**Figure S4.** Calculated bond distances in Å for (a) $TS_1$ ($D_{3d}$, $^1A_{1g}$) and (d) $TS_2$ ($D_{3h}$, $^1A_1'$) structures of $Rb_6Be_2B_6$ cluster, along with their (b/e) Wiberg bond indices (WBIs) and natural atomic charges (c/f; in |e|) from the natural bond orbital (NBO) analyses at the PBE0/def2-qzvp level.

**Figure S5.** Displacement vectors for the soft, imaginary vibrational modes of the $TS_1$ and $TS_2$ structures.

## Supplementary Information – Part II

**A short movie** extracted from the BOMD simulation for $Rb_6Be_2B_6$ cluster. The simulation was performed at 300 K for 20 ps. The movie roughly covers a time span of 6 ps.

**Figure S1.** Alternative optimized low-lying structures of $Rb_6Be_2B_6$ cluster. Relative energies are shown in square brackets at the PBE0/def2-qzvp level with corrections for zero-point energies (ZPEs). Also shown are the relative energies for top five isomers at the single-point CCSD(T)/def2-qzvp//PBE0/def2-qzvp level. All energies are in eV.

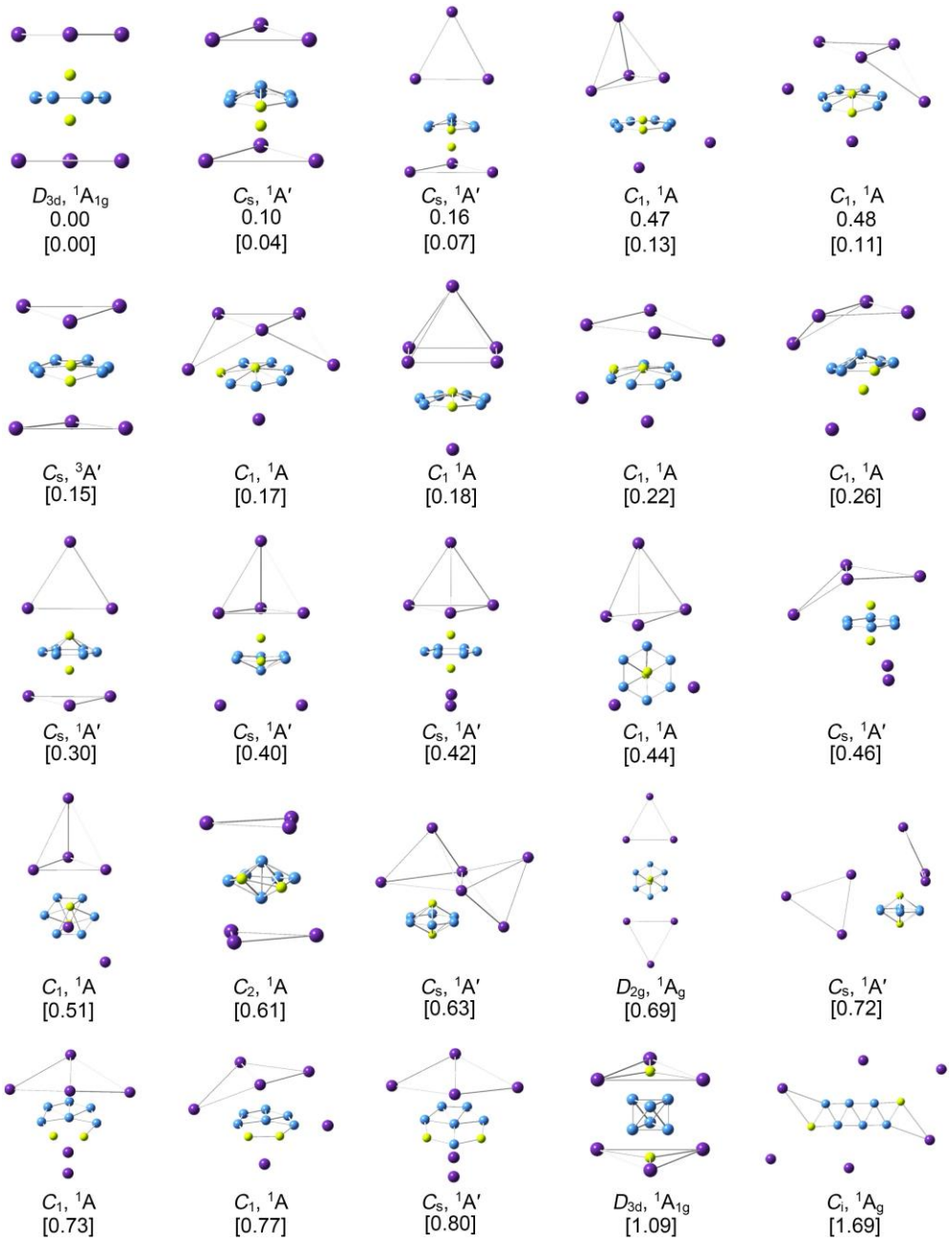

**Figure S2.** Two different σ bonding schemes for the $BeRb_3$ ligands in GM $D_{3d}$ ($^1A_{1g}$) $Rb_6Be_2B_6$ cluster on the basis of adaptive natural density partitioning (AdNDP) analysis. Occupation numbers (ONs) are indicated. The three-center two-electron (3c-2e) σ scheme in (b) gives a relatively low ON value, indicating that the σ bond is entirely delocalized within the tetrahedral $BeRb_3$ unit as presented in the 4c-2e σ scheme in (a).

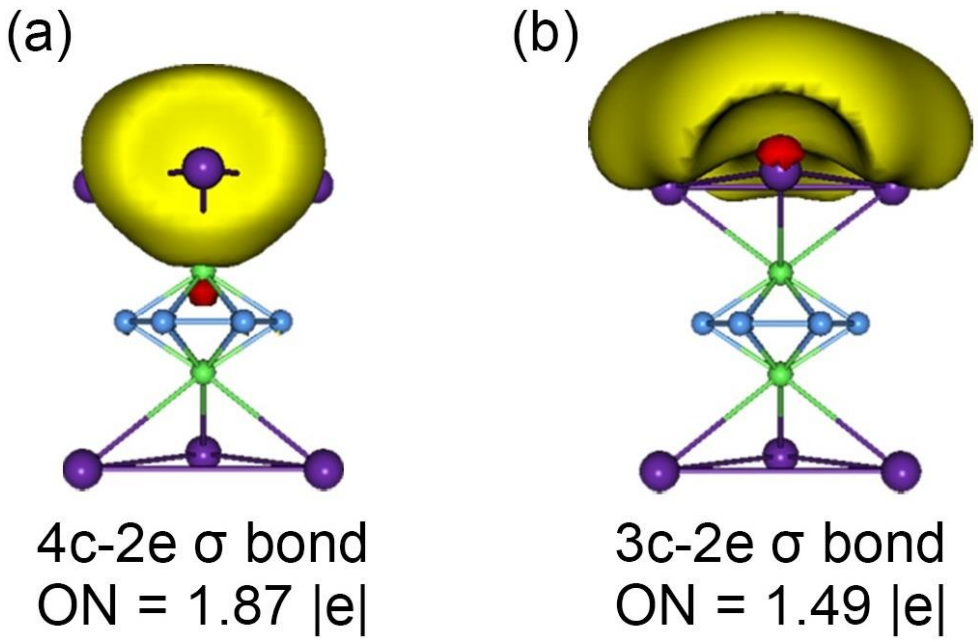

**Figure S3.** Comparison of the delocalized π/σ sextets of (a) $D_{3d}$ ($^1A_{1g}$) GM $Rb_6Be_2B_6$ cluster with those of (b) model $D_{6h}$ $C_6$ cluster and (c) benzene.

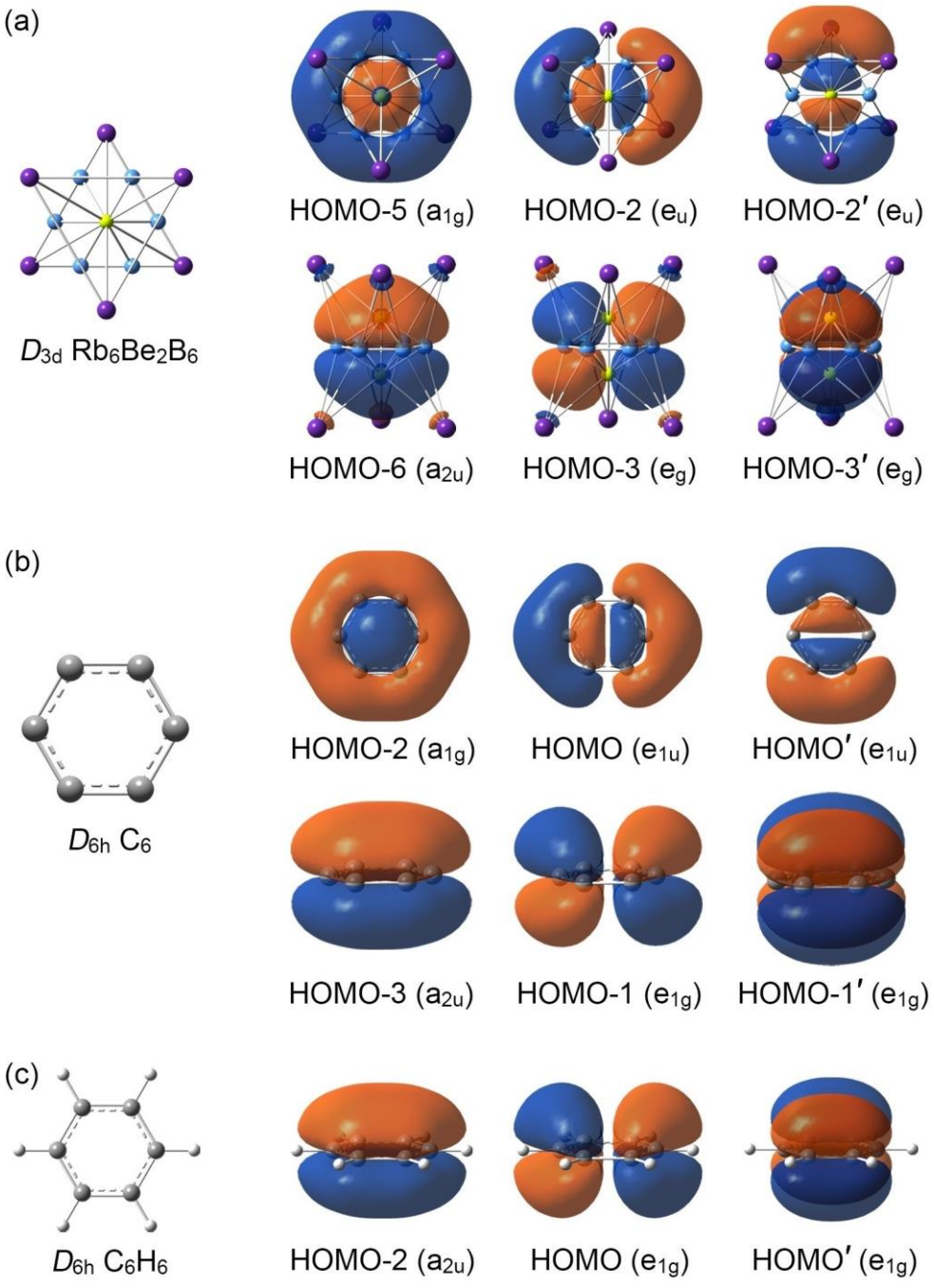

**Figure S4.** Calculated bond distances in Å for (a) $TS_1$ ($D_{3d}$, $^1A_{1g}$) and (d) $TS_2$ ($D_{3h}$, $^1A_1'$) structures of $Rb_6Be_2B_6$ cluster, along with their (b/e) Wiberg bond indices (WBIs) and natural atomic charges (c/f; in |e|) from the natural bond orbital (NBO) analyses at the PBE0/def2-qzvp level.

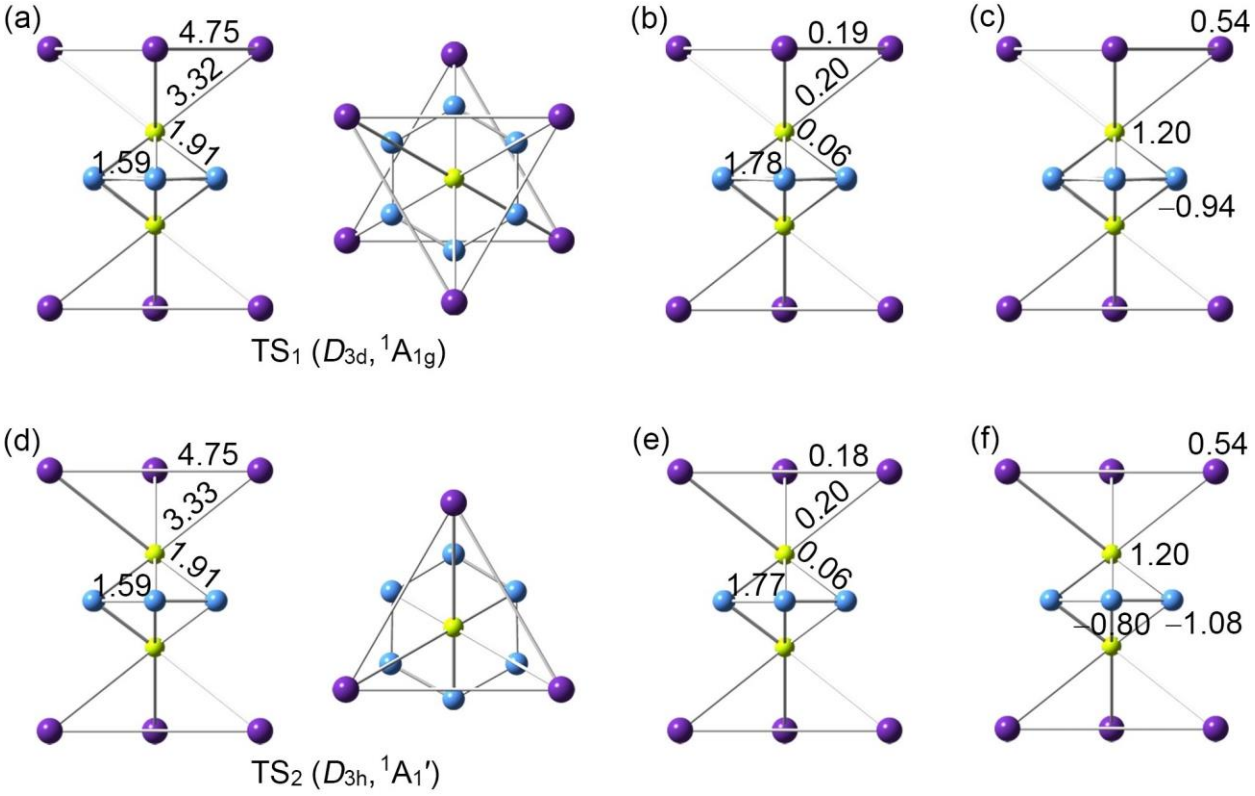

**Figure S5.** Displacement vectors for the soft, imaginary vibrational modes of the $TS_1$ and $TS_2$ structures.

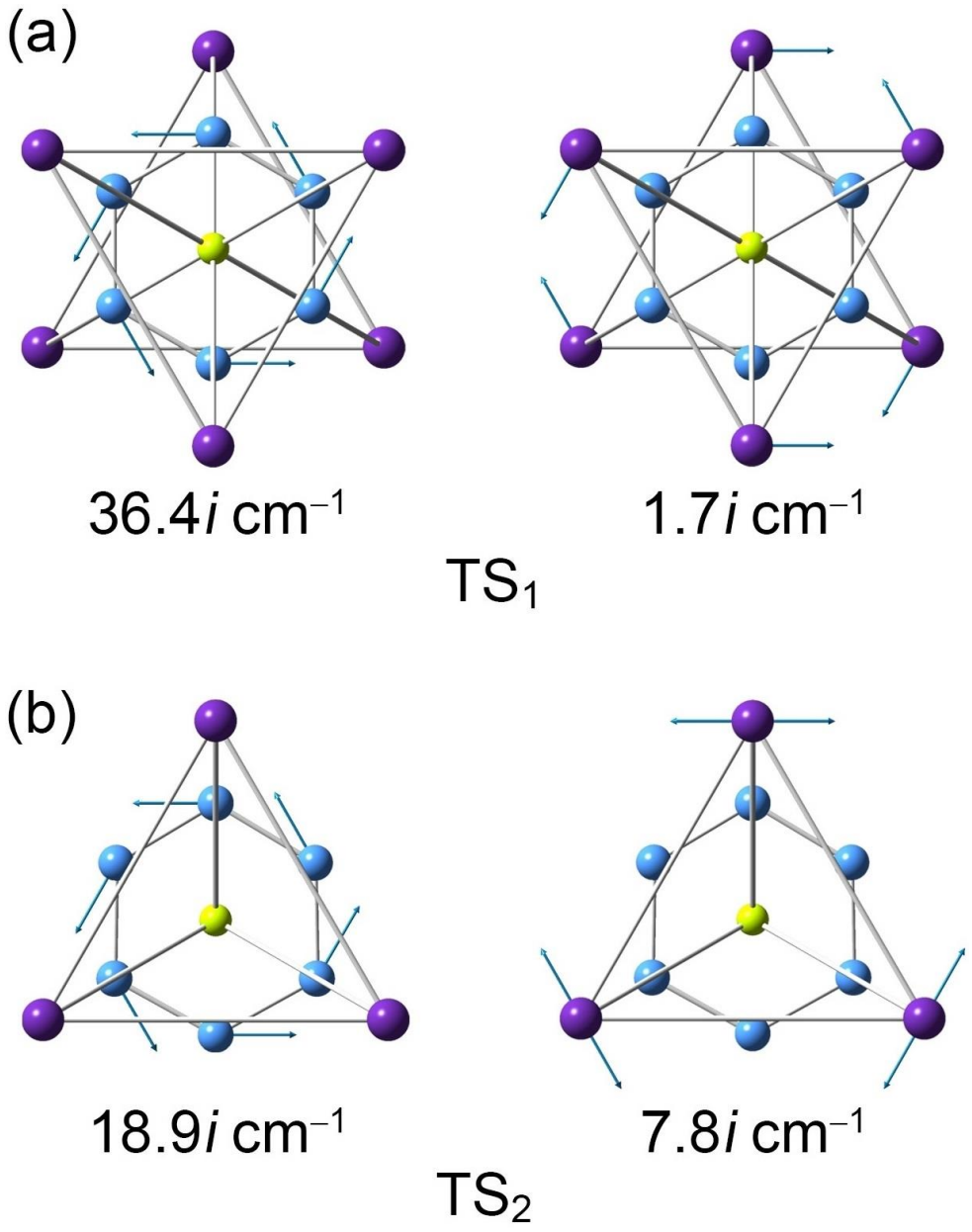

**Table S1.** Cartesian coordinates for selected optimized structures of $Rb_6Be_2B_6$ cluster at the PBE0/def2-qzvp level: the $D_{3d}$ ($^1A_{1g}$) global-minimum (GM) *versus* the $TS_1$ ($D_{3d}$, $^1A_{1g}$) and $TS_2$ ($D_{3h}$, $^1A_1'$) transition states (TSs).

**$Rb_6Be_2B_6$ GM ($D_{3d}$, $^1A_{1g}$)**

| | | | |
|---|---|---|---|
| B | 0.79666800 | 1.37986900 | 0.00000000 |
| B | -1.59333600 | 0.00000000 | 0.00000000 |
| B | -0.79666800 | 1.37986900 | 0.00000000 |
| B | 1.59333600 | 0.00000000 | 0.00000000 |
| B | 0.79666800 | -1.37986900 | 0.00000000 |
| B | -0.79666800 | -1.37986900 | 0.00000000 |
| Be | 0.00000000 | 0.00000000 | 1.04521700 |
| Be | 0.00000000 | 0.00000000 | -1.04521700 |
| Rb | -2.38064000 | -1.37446300 | -2.91883200 |
| Rb | 0.00000000 | 2.74892700 | -2.91883200 |
| Rb | 2.38064000 | -1.37446300 | -2.91883200 |
| Rb | 2.38064000 | 1.37446300 | 2.91883200 |
| Rb | 0.00000000 | -2.74892700 | 2.91883200 |
| Rb | -2.38064000 | 1.37446300 | 2.91883200 |

**$Rb_6Be_2B_6$ $TS_1$ ($D_{3d}$, $^1A_{1g}$)**

| | | | |
|---|---|---|---|
| B | 0.00000000 | 1.59235900 | 0.02400300 |
| B | -1.37902400 | -0.79618000 | 0.02400300 |
| B | -1.37902400 | 0.79618000 | -0.02400300 |
| B | 1.37902400 | 0.79618000 | -0.02400300 |
| B | 1.37902400 | -0.79618000 | 0.02400300 |
| B | 0.00000000 | -1.59235900 | -0.02400300 |
| Be | 0.00000000 | 0.00000000 | 1.04432700 |

| | | | |
|---|---|---|---|
| Be | 0.00000000 | 0.00000000 | -1.04432700 |
| Rb | -2.37331000 | -1.37023100 | -2.91919500 |
| Rb | 0.00000000 | 2.74046200 | -2.91919500 |
| Rb | 2.37331000 | -1.37023100 | -2.91919500 |
| Rb | 2.37331000 | 1.37023100 | 2.91919500 |
| Rb | 0.00000000 | -2.74046200 | 2.91919500 |
| Rb | -2.37331000 | 1.37023100 | 2.91919500 |

**$Rb_6Be_2B_6$ $TS_2$ ($D_{3h}$, $^1A_1'$)**

| | | | |
|---|---|---|---|
| B | 1.39248700 | 0.80395200 | 0.00000000 |
| B | -1.39248700 | 0.80395200 | 0.00000000 |
| B | 0.00000000 | 1.57697000 | 0.00000000 |
| B | 1.36569600 | -0.78848500 | 0.00000000 |
| B | 0.00000000 | -1.60790500 | 0.00000000 |
| B | -1.36569600 | -0.78848500 | 0.00000000 |
| Be | 0.00000000 | 0.00000000 | 1.04792800 |
| Be | 0.00000000 | 0.00000000 | -1.04792800 |
| Rb | -2.37416000 | 1.37072200 | -2.93360200 |
| Rb | 2.37416000 | 1.37072200 | -2.93360200 |
| Rb | 0.00000000 | -2.74144400 | -2.93360200 |
| Rb | 2.37416000 | 1.37072200 | 2.93360200 |
| Rb | 0.00000000 | -2.74144400 | 2.93360200 |
| Rb | -2.37416000 | 1.37072200 | 2.93360200 |